JOC*Article*

Azulene-Substituted Aromatic Amines. Synthesis and Amphoteric Redox Behavior of *N*,*N*-Di(6-azulenyl)-*p*-toluidine and *N*,*N*,*N*′,*N*′-Tetra(6-azulenyl)-*p*-phenylenediamine and Their Derivatives

Shunji Ito,*,† Takahiro Kubo,‡ Noboru Morita,‡ Tadaaki Ikoma,§ Shozo Tero-Kubota,§ Jun Kawakami,† and Akio Tajiri†

Department of Materials Science and Technology, Faculty of Science and Technology, Hirosaki University, Hirosaki 036-8561, Department of Chemistry, Graduate School of Science, Tohoku University, Sendai 980-8578, and Institute of Multidisciplinary Research for Advanced Materials, Tohoku University, Sendai 980-8577, Japan

itsnj@cc.hirosaki-u.ac.jp

Received August 28, 2004

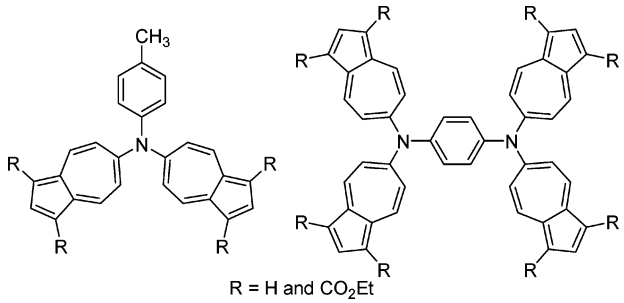

N,*N*-Di(6-azulenyl)-*p*-toluidine (**1a**) and *N*,*N*,*N*′,*N*′-tetra(6-azulenyl)-*p*-phenylenediamine (**2a**) and their derivatives with 1,3-bis(ethoxycarbonyl) substituents on each 6-azulenyl group (**1b** and **2b**) were prepared by Pd-catalyzed amine azulenylation and characterized as a study into new aromatic amines for multistage amphoteric redox materials. The redox behavior of each compound was characterized by cyclic voltammetry. These compounds undergo facile reduction to stable anion radicals and dianion diradicals owing to the resonance stabilization between the 6-azulenyl groups and exhibit electrochemical oxidation depending on the amine subunits. The ESR measurement of anion radicals and a dianion diradical generated by the electrochemical reduction of amine **1b** and diamine **2b** revealed that the unpaired electron of these radicals delocalizes over the entire azulene ring including the central nitrogen atoms. UV−vis spectral analysis of amines **1a**,**b** and diamines **2a**,**b**, taken during the electrochemical reduction, exhibited a gradual decrease of the absorption bands of the neutral species along with an increase of the new absorption maxima at 625, 605, 640, and 610 nm, respectively, with the development of well-defined isosbestic points at 502, 562, 478, and 545 nm, respectively. As indicated by a combined ESR and UV−vis spectral study, the species giving rise to the new absorption maxima are concluded to be the generation of anion radicals and dianion diradicals of aromatic amines and diamines with high thermodynamic stability.

Introduction

Recently, polyaromatic amines have been of great interest owing to their potential applications in electrochemical devices such as hole transport materials for organic light-emitting diodes because of their properties to undergo facile oxidation to stable cation radicals.[1] Indeed, *p*-phenylenediamine derivatives studied earlier produce stabilized positive radical ions (Scheme 1).[2] However, negative radical ions of aromatic amines, in which the amino group is an electron donor, are paid little attention due to the lower stability of the species. An ESR study of the anion radical of 1-phenylethylamine reports it as an unstable intermediate.[3] Electrochemical reduction of 9-aminofluorene gives an anion radical to decom-

* To whom correspondence should be addressed. Phone: +81-172-39-3568. Fax: +81-172-39-3541.
† Hirosaki University.
‡ Graduate School of Science, Tohoku University.
§ Institute of Multidisciplinary Research for Advanced Materials, Tohoku University.

10.1021/jo048489s CCC: $30.25
Published on Web 02/16/2005

SCHEME 1

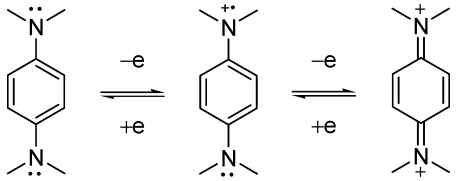

pose by carbon−nitrogen bond cleavage.[4] Unstable lithium 1-(dimethylamino)naphthalenide reagent is developed for the reductive lithiation reaction.[5]

Azulene ($C_{10}H_8$) has attracted the interest of many research groups due to its unusual properties as well as its beautiful blue color.[6] Especially, the azulene system has a tendency to stabilize cations, as well as anions, owing to its remarkable polarizability. We have recently reported that substitution of azulenes at the 6-position induces facile electrochemical reduction to provide stabilized anionic species.[7] In addition to the property of aromatic amines to exhibit facile oxidation, the electronic property of azulene would provide an opportunity to construct aromatic amines with high amphoteric redox properties. In recent years, a number of Pd(0)-catalyzed cross-coupling reactions of aryl halides[8] or triflates[9] with amines have been reported. We have also reported the Pd(0)-catalyzed reaction of 2-bromoazulene with several alkyl and aromatic amines to afford 2-aminoazulene derivatives.[10] In the search for new potential multistage amphoteric redox compounds we have prepared and characterized *N*,*N*-di(6-azulenyl)-*p*-toluidine (**1a**) and *N*,*N*,*N*′,*N*′-tetra(6-azulenyl)-*p*-phenylenediamine (**2a**) and their derivatives with 1,3-bisethoxycarbonyl substituents on each 6-azulenyl group (**1b** and **2b**) using Pd(0)-catalyzed amine azulenylation (Chart 1).

CHART 1

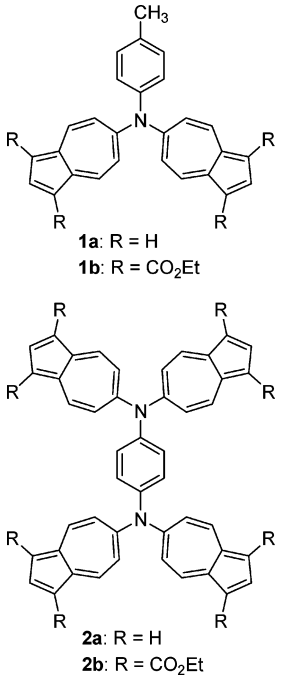

Construction of organic molecules that contain multiple redox-active chromophores is also fairly important for the preparation of novel polyelectrochromic materials, which respond to different potentials with a variety of colors.[11] Due to the substitution of azulenyl groups, the azulene-substituted aromatic amines should also exhibit novel polyelectrochromic behavior. We also report herein the electrochromic behavior of the azulene-substituted aromatic amines.

Results and Discussion

Synthesis. The preparation of azulene-substituted aromatic amines was accomplished by the Pd(0)-catalyzed cross-coupling reaction of 6-bromoazulenes **3a** and **3b**[12] with *p*-toluidine (**4**) and *p*-phenylenediamine (**6**) (Schemes 2 and 3). The reaction conditions were optimized utilizing the reaction of diethyl 6-bromoazulene-1,3-dicarboxylate (**3b**) with **4** to afford *N*,*N*-bis(1,3-bisethoxycarbonyl-6-azulenyl)-*p*-toluidine (**1b**). The results are summarized in Table 1. The reaction of **3b** with several nucleophiles proceeds without any catalyst due to the high efficiency of the 6-position of the azulene ring toward the electrophiles.[13] However, the reaction of **3b** with **4** in toluene did not afford any products both at room temperature and at 80 °C without Pd catalyst (entries 1 and 5). The Pd(0)-catalyzed reaction of **3b** with **4** at room temperature afforded *N*-(1,3-bisethoxycarbonyl-6-azulenyl)-*p*-toluidine (**5b**) in high yield without significant

(1) See e.g.: (a) Thelakkat, M.; Schmidt, H.-W. *Adv. Mater.* **1998**, *10*, 219−223. (b) Wang, J.-F.; Kawabe, Y.; Shaheen, S. E.; Morrell, M. M.; Jabbour, G. E.; Lee, P. A.; Anderson, J.; Armstrong, N. R.; Kippelen, B.; Mash, E. A.; Peyghambarian, N. *Adv. Mater.* **1998**, *10*, 230−233. (c) Okumoto, K.; Shirota, Y. *Chem. Lett.* **2000**, 1034−1035. (d) Shirota, Y.; Kinoshita, M.; Noda, T.; Okumoto, K.; Ohara, T. *J. Am. Chem. Soc.* **2000**, *122*, 11021−11022. (e) Okamoto, T.; Terada, E.; Kozaki, M.; Uchida, M.; Kikukawa, S.; Okada, K. *Org. Lett.* **2003**, *5*, 373−376. (f) Li, Z. H.; Wong, M. S.; Tao, Y.; D'Iorio, M. *J. Org. Chem.* **2004**, *69*, 921−927.

(2) Deuchert, K.; Hünig, S. *Angew. Chem., Int. Ed. Engl.* **1978**, *17*, 875−886.

(3) Eloranta, J.; Kolehmainen, E. *Suom. Kemistil. B* **1973**, *46*, 271−273.

(4) Barnes, J. H.; Triebe, F. M.; Hawley, M. D. *J. Electroanal. Chem.* **1982**, *139*, 395−411.

(5) Cohen, T.; Guo, B.-S. *Tetrahedron* **1986**, *42*, 2803−2808.

(6) Zeller, K.-P. Azulene. In *Houben-Weyl: Methoden der Organischen Chemie*, 4th ed.; Georg Thieme: Stuttgart, Germany, 1985; Vol. V, Part 2C, pp 127−418.

(7) (a) Ito, S.; Inabe, H.; Okujima, T.; Morita, N.; Watanabe, M.; Harada, N.; Imafuku, K. *J. Org. Chem.* **2001**, *66*, 7090−7101. (b) Ito, S.; Okujima, T.; Morita, N. *J. Chem. Soc., Perkin Trans. 1* **2002**, 1896−1905. (c) Ito, S.; Inabe, H.; Morita, N.; Ohta, K.; Kitamura, T.; Imafuku, K. *J. Am. Chem. Soc.* **2003**, *125*, 1669−1680.

(8) See e.g.: (a) Wolfe, J. P.; Wagaw, S.; Buchwald, S. L. *J. Am. Chem. Soc.* **1996**, *118*, 7215−7216. (b) Driver, M. S.; Hartwig, J. F. *J. Am. Chem. Soc.* **1996**, *118*, 7217−7218. (c) Wolfe, J. P.; Buchwald, S. L. *J. Org. Chem.* **1997**, *62*, 6066−6068. (d) Hartwig, J. F.; Kawatsura, M.; Hauck, S. I.; Shaughnessy, K. H.; Alcazar-Roman, L. M. *J. Org. Chem.* **1999**, *64*, 5575−5580. (e) Yang, B. H.; Buchwald, S. L. *J. Organomet. Chem.* **1999**, *576*, 125−146. (f) Wolfe, J. P.; Tomori, H.; Sadighi, J. P.; Yin, J.; Buchwald, S. L. *J. Org. Chem.* **2000**, *65*, 1158−1174.

(9) (a) Wolfe, J. P.; Buchwald, S. L. *J. Org. Chem.* **1997**, *62*, 1264−1267. (b) Louie, J.; Driver, M. S.; Hamann, B. C.; Hartwig, J. F. *J. Org. Chem.* **1997**, *62*, 1268−1273.

(10) Yokoyama, R.; Ito, S.; Okujima, T.; Kubo, T.; Yasunami, M.; Tajiri, A.; Morita, N. *Tetrahedron* **2003**, *59*, 8191−8198.

(11) (a) Monk, P. M. S.; Mortimer, R. J.; Rosseninsky, D. R. *Electrochromism: Fundamentals and Applications*; VCH: Weinheim, Germany, 1995. (b) Komatsu, T.; Ohta, K.; Fujimoto, T.; Yamamoto, I. *J. Mater. Chem.* **1994**, *4*, 533−536. (c) Rosseinsky, D. R.; Monk, D. M. S. *J. Appl. Electrochem.* **1994**, *24*, 1213−1221.

(12) McDonald, R. N.; Richmond, J. M.; Curtis, J. R.; Petty, H. E.; Hoskins, T. L. *J. Org. Chem.* **1976**, *41*, 1811−1821.

(13) Nozoe, T.; Takase, K.; Tada, M. *Bull. Chem. Soc. Jpn.* **1965**, *38*, 247−251.

SCHEME 2

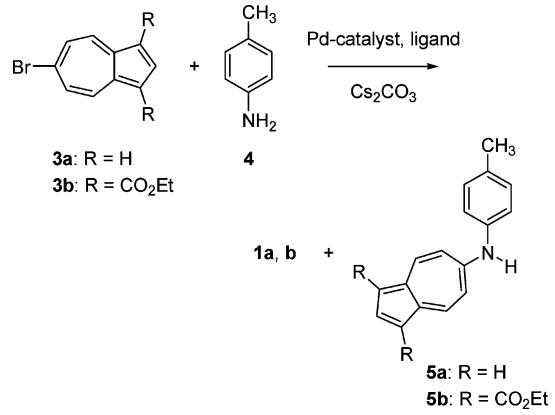

SCHEME 3

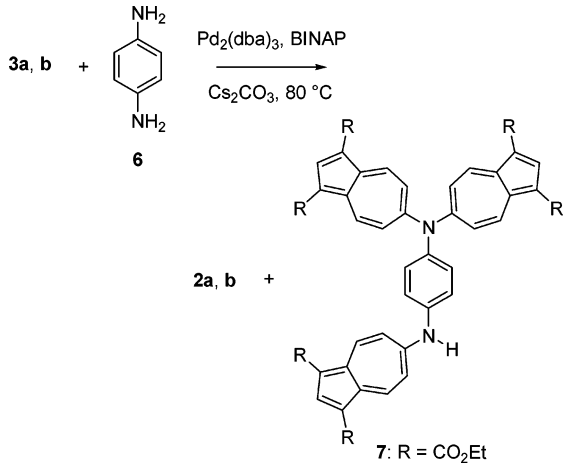

TABLE 1. Pd-Catalyzed Reaction of 3b with *p*-Toluidine (4)[a]

					yield[b]/%		
entry	catalyst	ligand	temp	time/d	**5b**	**1b**	recovered **3b**
1			rt	2			91
2	$Pd(PPh_3)_4$		rt	2	67		33
3	$Pd_2(dba)_3$	BINAP[c]	rt	2	73	9	34
4	$Pd_2(dba)_3$	P(*o*-Tol)$_3$	rt	2	78		41
5			80 °C	1			82
6	$Pd(PPh_3)_4$		80 °C	1	29	33	
7	$Pd_2(dba)_3$	BINAP	80 °C	1	9	66	
8	$Pd_2(dba)_3$	P(*o*-Tol)$_3$	80 °C	1	81	11	

[a] The reactions of **3b** (0.4 mmol) with **4** (0.2 mmol) were carried out by using 10 mol % Pd(0) catalyst, ligand (Pd:P = 1:2), and Cs_2CO_3 (1.3 mmol) in toluene (10 mL). [b] All yields are isolated yields and are an average of two runs. The yields of **5b** are calculated on the basis of the amount of **4** used. [c] BINAP = 2,2′-bis(diphenylphosphino)-1,1′-binaphthyl.

difference with various Pd catalysts used (entries 2−4). The Pd-catalyzed reaction of **3b** with **4** at 80 °C gave the expected **1b** (entries 6−8). However, the choice of the catalytic system is important to produce **1b** in good yield. The use of $Pd(PPh_3)_4$ as a catalyst was ineffective in this reaction (entry 6). Substitution of the $Pd(PPh_3)_4$ catalyst with $Pd_2(dba)_3$−BINAP as a catalyst resulted in a significant increase of the desired product **1b** in 66% yield (entry 7). The yield of **1b** was not improved by the use of the $Pd_2(dba)_3$−P(*o*-Tol)$_3$ catalytic system (entry 8), which was the most effective catalytic system for the production

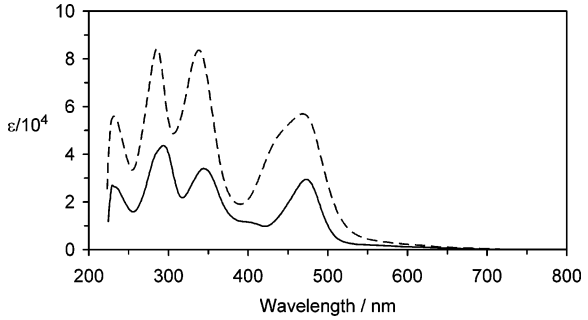

FIGURE 1. UV−vis spectra of amine **1a** (solid line) and diamine **2a** (broken line) in dichloromethane.

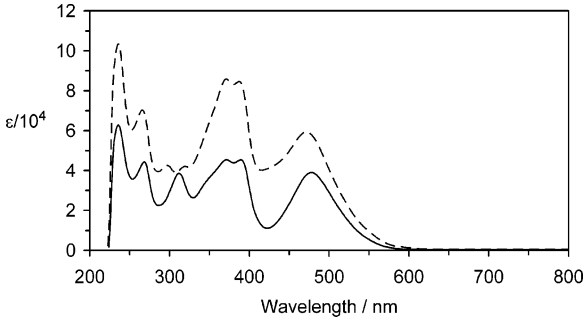

FIGURE 2. UV−vis spectra of amine **1b** (solid line) and diamine **2b** (broken line) in dichloromethane.

of **5b** at room temperature. Compound **5b** reacted with **3b** to give **1b** in 75% yield under the $Pd_2(dba)_3$−BINAP reaction conditions.

The Pd(0)-catalyzed reaction of 6-bromoazulene (**3a**) with **4** was conducted under the $Pd_2(dba)_3$−BINAP reaction conditions. The reaction of **3a** afforded **1a** in 52% yield along with *N*-(6-azulenyl)-*p*-toluidine (**5a**) (35%) (Scheme 2). By the use of **6** as an amine instead of **4**, the expected products *N*,*N*,*N*′,*N*′-tetra(6-azulenyl)-*p*-phenylenediamines **2a** and **2b** were obtained in 20% yields under the $Pd_2(dba)_3$−BINAP reaction conditions along with tris adduct **7** in 15% yield in the case of the reaction of **3b** (Scheme 3). These compounds were obtained as stable crystals with acceptable solubility for application and were fully characterized by spectroscopic data (see the Experimental Section). However, amine **1a** and diamine **2a** exhibited some decomposition during the prolonged ^{13}C NMR measurements probably due to the contaminant acid in $CDCl_3$.

UV−vis spectra of amines **1a**,**b** and diamines **2a**,**b** in dichloromethane are shown in Figures 1 and 2. Azulene-substituted aromatic amines **1a**,**b** exhibit a strong absorption in the visible region [λ_{max} (nm) (ϵ): **1a**, 472 (29300); **1b**, 478 (38900)]. The absorption maxima of the UV−vis spectra of azulene-substituted *p*-phenylenediamines **2a**,**b** [λ_{max} (nm) (ϵ): **2a**, 469 (56900); **2b**, 472 (59000)] are observed in a wavelength region similar to those of **1a**,**b**. The absorption maxima of **2a**,**b** showed only blue shifts by 3 and 6 nm, respectively, compared with those of **1a**,**b**. The absorption coefficients of diamines **2a**,**b** are almost twice as large as those of **1a**,**b**. This indicates a small interaction between the two di(6-azulenyl)amine units in diamines **2a**,**b**. To obtain the characteristic features of the UV−vis spectra, the molecular orbitals of amine **1a** without a 4′-methyl sub-

TABLE 2. Redox Potentials of Amines 5a,b and 1a,b and Diamines 2a,b[a]

sample	E_1^{red}	E_2^{red}	E_3^{red}	E_1^{ox}	E_2^{ox}	E_3^{ox}	E_4^{ox}	E_5^{ox}
5a	(−2.08)			(+0.46)	(+1.41)			
5b	(−1.73)			(+0.87)	(+1.51)			
1a	−1.77	(−2.12)		(+0.57)	(+0.89)	(+1.15)	(+1.57)	(+2.10)
1b	−1.32	(−1.70)		(+1.02)	(+1.42)			
2a	−1.76 (2e)	(−2.07)	(−2.18)	(+0.50)	(+0.84)	(+1.14)	(+1.57)	(+2.21)
2b	−1.31 (2e)	(−1.61)	(−1.74)	(+0.91)	(+1.06)	(+1.39)	(+1.63)	

[a] The redox potentials were measured by CV or DPV (V vs Ag/Ag^+, 0.1 M Et_4NClO_4 in benzonitrile, Pt electrode, scan rate 100 mV s^{-1}, and $Fc/Fc^+ = 0.16$ V). In the case of irreversible waves, which are shown in parentheses, E_{ox} and E_{red} were calculated as E_{pa} (anodic peak potential) − 0.03 V and E_{pc} (cathodic peak potential) + 0.03 V, respectively.

stituent were examined by B3LYP/6-31G** density functional calculation.[14] The optimized structures with HOMOs and LUMOs are shown in the Supporting Information. The HOMO and the HOMO − 1 are delocalized over the two azulenyl groups; however, HOMO − 2, which is located at almost the same energy level as HOMO − 1, is delocalized over the whole molecule including the central nitrogen atom. On the other hand, the LUMO is delocalized over two azulenyl groups. The examination of the HOMOs and the LUMO indicates that the absorption results in a charge transfer from the *p*-toluidine moiety to the azulene ring. The HOMO−LUMO transition should be assigned to the weak shoulder at the longest wavelength region around 580 nm in the UV−vis spectra of **1a** and **2a**. Any fluorescence emission was not observed for amine **1b** and diamine **2b** in dichloromethane due to the substitution of several azulenyl groups.

Cyclic Voltammetry. To clarify the electrochemical property, the redox behavior of amines **1a**,**b** and **5a**,**b** and diamines **2a**,**b** was examined by cyclic voltammetry (CV) and differential pulse voltammetry (DPV). Measurements were made using a standard three-electrode configuration. Tetraethylammonium perchlorate (0.1 M) in benzonitrile was used as a supporting electrolyte with platinum wire auxiliary and working electrodes. All measurements were carried out under an argon atmosphere, and potentials were related to the reference electrode formed by Ag/Ag^+ and using as internal reference Fc/Fc^+ which discharges at +0.16 V. Redox potentials (V vs Ag/Ag^+) of amines **1a**,**b** and **5a**,**b** and diamines **2a**,**b** are summarized in Table 2. The reduction waves of amines **1a**,**b** and diamines **2a**,**b** are shown in Figures 3 and 4. The reduction waves of amines **5a**,**b** and the oxidation waves of amines **1a**,**b** and **5a**,**b** and diamines **2a**,**b** are shown in the Supporting Information.

Amine **5a** exhibited an irreversible reduction wave at −2.08 V depending on the reduction of the 6-azulenyl substituent. Similar to the redox behavior of **5a**, amine **5b** also showed an irreversible reduction wave at −1.73 V in the cyclic voltammogram. Thus, the ethoxycarbonyl groups substituted in the five-membered ring increase

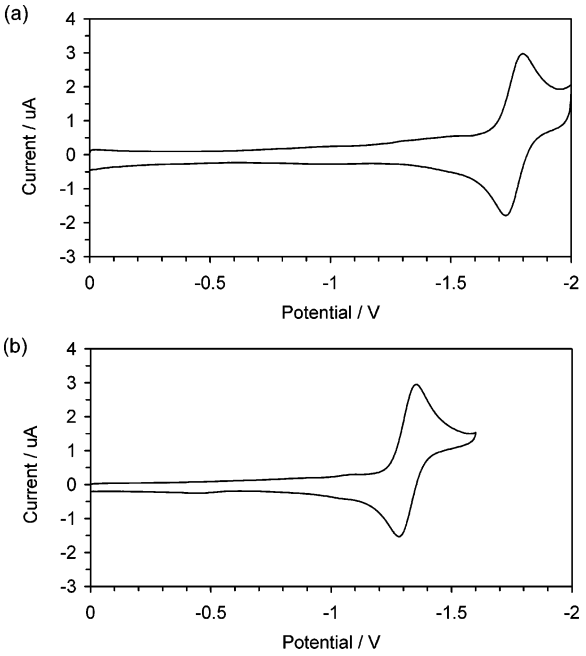

FIGURE 3. Cyclic voltammograms of (a) amine **1a** (1 mM) and (b) amine **1b** (1 mM) in benzonitrile containing Et_4NClO_4 (0.1 M) as a supporting electrolyte.

the electron affinity by 0.35 V. In contrast to the irreversible reduction wave of amines **5a**,**b**, amines **1a**,**b** exhibited a reduction wave with high reversibility (**1a**, −1.77 V; **1b**, −1.32 V) and an irreversible wave (**1a**, −2.12 V; **1b**, −1.70 V) in the cyclic voltammogram depending on the reduction of two 6-azulenyl substituents (Scheme 4). The less negative E_1^{red} potentials of **1a**,**b** compared with **5a**,**b** and the improvement of reversibility of the E_1^{red} waves are attributable to the stabilization of the radical anionic state by introducing the two 6-azulenyl groups. The E_2^{red} values of **1a**,**b** are almost comparable with the E_1^{red} values of **5a**,**b**.

The electrochemical reduction of diamines **2a**,**b** exhibited a three-step reduction wave. A quantitative evaluation of the first reduction wave in Figure 4 exhibits more current compared with those of amines **1a**,**b** in Figure 3 in the same concentration. Furthermore, the next two small waves compared with the first reduction wave of diamines **2a**,**b** (see the Supporting Information) afford evidence that the three-step reduction is characterized as a two-electron reduction wave following two one-electron processes (Scheme 5). The E_1^{red} potentials of diamines **2a**,**b** at −1.76 and −1.31 V, respectively, are almost comparable with those of amines **1a**,**b**. The E_2^{red} and E_3^{red} values of **2a**,**b** are almost comparable with the

(14) The molecular orbital calculations were done with a Gaussian revision E.2 program package, which was installed in a UNIX workstation under a molecular design support system in IMRAM: Frisch, M. J.; Trucks, G. W.; Schlegel, H. B.; Gill, P. M. W.; Johnson, B. G.; Robb, M. A.; Cheeseman, J. R.; Keith, T.; Petersson, G. A.; Montgomery, J. A.; Raghavachari, K.; Al-Laham, M. A.; Zakrzewski, V. G.; Ortiz, J. V.; Foresman, J. B.; Cioslowski, J.; Stefanov, B. B.; Nanayakkara, A.; Challacombe, M.; Peng, C. Y.; Ayala, P. Y.; Chen, W.; Wong, M. W.; Andres, J. L.; Replogle, E. S.; Gomperts, R.; Martin, R. L.; Fox, D. J.; Binkley, J. S.; Defrees, D. J.; Baker, J.; Stewart, J. P.; Head-Gordon, M.; Gonzalez, C.; Pople, J. A. *Gaussian*, revision E.2; Gaussian, Inc.: Pittsburgh, PA, 1995.

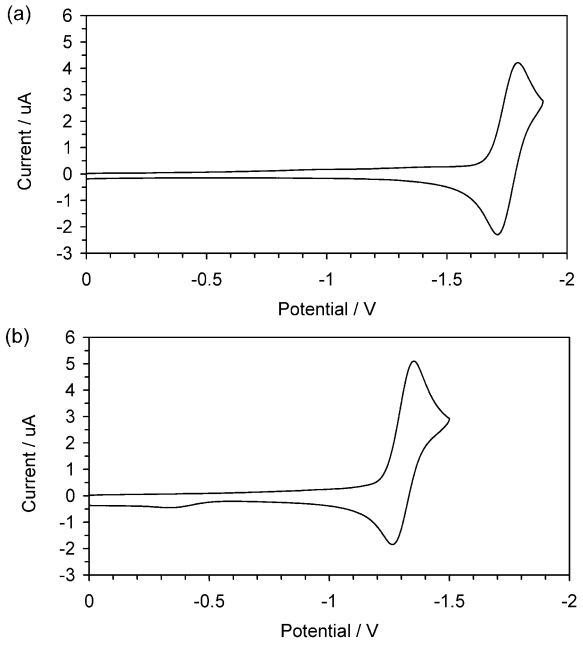

FIGURE 4. Cyclic voltammograms of (a) diamine **2a** (1 mM) and (b) diamine **2b** (1 mM) in benzonitrile containing Et_4NClO_4 (0.1 M) as a supporting electrolyte.

E_2^{red} values of **1a**,**b**. These results indicate that there is no significant electrochemical interaction between the two di(6-azulenyl)amine units in diamines **2a**,**b**. Therefore, the two di(6-azulenyl)amino substituents on a benzene ring in a 1,4 relationship increase the multiplicity of the electron-accepting properties.

The oxidation waves are irreversible in all cases at 100 mV s^{-1} owing to the destabilization arising from the electron-withdrawing 6-azulenyl substituents. The oxidation of amines **5a**,**b** exhibited a two-step wave. The E_1^{ox} wave should correspond to the electron removal from the arylamino group, forming cation radicals. The removal of the second electron from the cation radicals correspond to the redox reaction of the substituted 6-azulenyl group. The E_1^{ox} potentials of amines **1a**,**b** are slightly more positive compared with those of **5a**,**b** due to the electron-withdrawing nature of the 6-azulenyl groups. Cation radicals of azulenes are not persistent without any substituents on the reactive C-1 and C-3 positions.[15] Thus, the multiple electron transfer of amine **1a** on further oxidation is probably due to the decomposition of the oxidized species. The oxidation behavior of diamine **2a** is more or less similar to that of amine **1a**, although diamine **2a** slightly decreases the E_1^{ox} potential. The electrochemical oxidation of diamine **2b** exhibited four irreversible oxidation stages corresponding to the two oxidizable nitrogen centers and four 6-azulenyl groups to generate the polycationic species. The redox property of these compounds is ascribed to the stabilization of the radical anionic states of amines by the resonance effect with 6-azulenyl groups, although the electron-withdrawing nature of the groups decreases the stability of the radical cationic states.

SCHEME 5

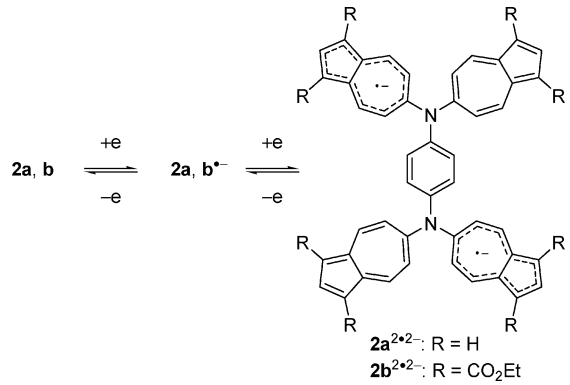

ESR Measurements. Anion radicals **1b**$^{\bullet-}$ and **2b**$^{\bullet-}$ and dianion diradical **2b**$^{2\bullet2-}$ were characterized by ESR measurements, which were carried out at room temperature with use of a degassed dimethylformamide solution prepared under a vacuum line containing tetrapropylammonium perchlorate as a supporting electrolyte. For the measurements under electrolysis, we used a two-electrode apparatus. In most cases it is necessary to increase the potentials for the presumed redox reaction compared with those obtained by CV. The redox reaction was monitored by the color change of the solution.

SCHEME 4

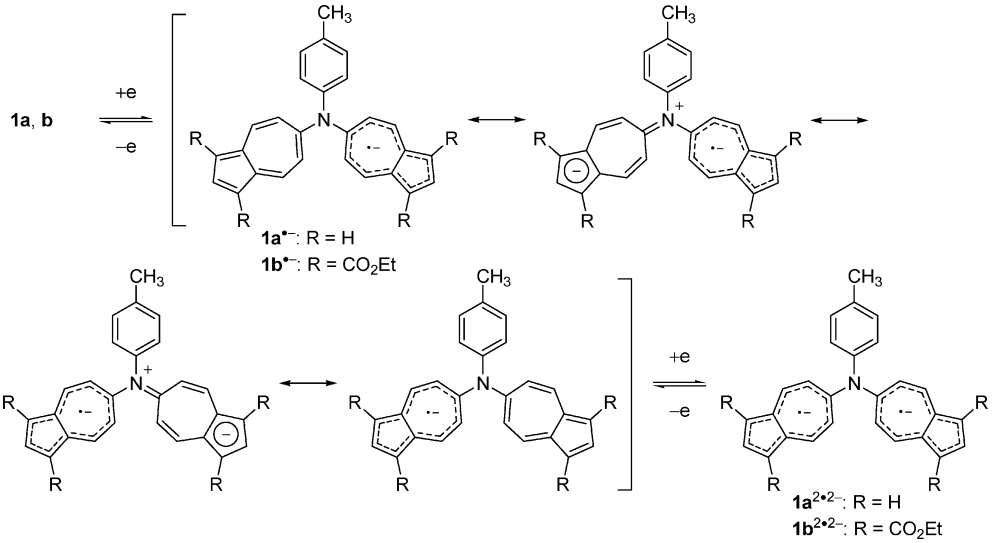

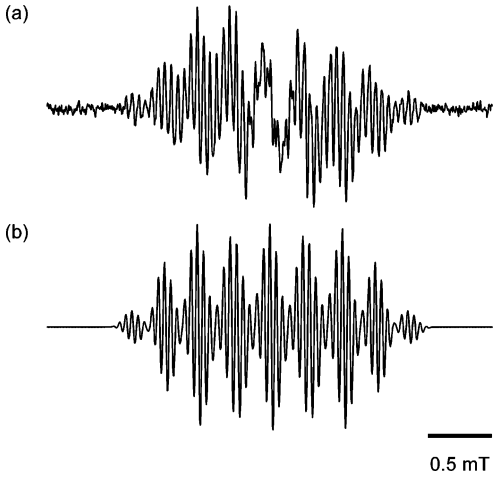

FIGURE 5. ESR spectrum of radical anion **1b**$^{\bullet-}$ generated by the electrochemical reduction in dimethylformamide at room temperature: (a) observed ESR spectrum and (b) computer simulation.

The red solution of amine **1b** did not indicate any ESR signal, but the multiline ESR in Figure 5a appeared with the color change to green during the electrochemical reduction. This fact indicates that the green color originates from the radical anionic species **1b**$^{\bullet-}$. According to the line width difference of each line, the observed spectrum consists of two components which are the main signals expanded in a wide field of 2.4 mT and the sharp signals gathering in the central field. On the basis of the signal intensity, we assigned the main signals to anion radical **1b**$^{\bullet-}$ and the central component to paramagnetic byproducts generated during the electrolysis. From the pattern of the outermost groups in the main spectrum of **1b**$^{\bullet-}$**,** which offers useful information about the smallest coupling constant among many hyperfine splittings, it can be recognized that the main signals have septet lines with an intensity ratio of 1:6:15:20:15:6:1. This pattern is interpreted in terms of the hyperfine splittings due to six protons with a small coupling constant of 0.048 mT. Moreover, in the spectrum of **1b**$^{\bullet-}$, this septet pattern is roughly repeated nine times with an intensity ratio of 1:4:7:8:8:8:7:4:1, although the spectral overlap with the byproducts makes the splitting pattern in the central group unclear. Nine such groups of septet lines could be totally simulated by employing the additional hyperfine splittings due to a nitrogen atom with a coupling constant of ca. 0.6 mT and four equivalent protons with a coupling constant of ca. 0.3 mT. Figure 5b exhibits the best simulation spectrum calculated with an optimized parameter set with a g value of 2.0025 and coupling constants of 0.572 (1N), 0.257 (4H), and 0.048 mT (6H).

We have performed a B3LYP/6-31G** density functional calculation to estimate the spin density distribution of anion radical **1b**$^{\bullet-}$ without any substituents. The calculated structure of the anion radical does not show significant alteration compared with that of the neutral species in their geometry, although slight changes in the dihedral angles of the rings from the central planar nitrogen atom are observed (see the Supporting Information). The spin density distributions calculated for the anion radical are characterized by the high π-spin density at the 2-, 3a-, 4-, 6-, 8-, 8a-carbons and the central nitrogen and low density at the 1-, 3-, 5-, and 7-carbons on each azulene ring. Therefore, the observed ESR spectrum should be explained by the hyperfine interactions with a nitrogen atom in the amino group and four 4,8-protons and six 2,5,7-protons on each azulene ring (Chart 2). Thus, the ESR studies for the anion radical revealed that the unpaired electron delocalizes over the two azulene rings including the central nitrogen atom.

The ESR measurement of diamine **2b** under electrochemical reduction conditions was characterized by two different ESR spectra depending on the reduction potentials applied. The multiline ESR spectrum in Figure 6a was observed by the electrochemical reduction of **2b** at −1.5 V. Compared with the spectrum of amine anion radical **1b**$^{\bullet-}$, the line number increases and the intensity distribution becomes more bell shaped. This is qualitatively understood by an increase in the number of interacting magnetic nuclei. Because diamine **2b** has more protons and nitrogen atoms than amine **1b**, the observed bell-shaped spectrum is safely assigned to radical anion **2b**$^{\bullet-}$. Under these electrolysis conditions, weak septet lines were also detected at the edges of the main spectrum. The line width of these satellite lines is broader than that of the main signals, and their line positions coincide with the terminal groups of lines in the spectrum of dianion diradical **2b**$^{2\bullet2-}$ described later. Hence, it is concluded that the weak septet lines are attributed to a small number of **2b**$^{2\bullet2-}$ dianion diradicals which are present in equilibrium with **2b**$^{\bullet-}$ under the reductive atmosphere. The simulation for the spectrum of **2b**$^{\bullet-}$ is shown in Figure 6b. The ESR parameters used for the simulation are a g value of 2.0025 and hyperfine coupling constants of 0.207 (2N), 0.125 (8H), and 0.024 mT (12H). All the noticeable lines are reproduced using these parameters, although the intensity distribution of the simulation is slightly deviated from the observed one. The disagreement in intensity may be caused by the broad signals due to **2b**$^{2\bullet2-}$ underneath the main spectrum of **2b**$^{\bullet-}$. To compare the obtained coupling constants with the calculated spin density distribution, we have also performed a B3LYP/6-31G** density functional calculation of **2b**$^{\bullet-}$ without ester substituents. The optimized structure is shown in the Supporting Information. The calculation revealed that the spin density of the radical anion distributes over all four azulene rings (Chart 2). Therefore, the obtained coupling constants are reasonably interpreted in terms of the hyperfine interactions with two nitrogen atoms in the amino groups and eight 4,8-protons and twelve 2,5,7-protons on each azulene ring. It was clarified that the unpaired electron in **2b**$^{\bullet-}$ delocalizes over all four azulene rings including the two nitrogen atoms.

When diamine **2b** was reduced under −3.0 V, the ESR spectrum due to **2b**$^{\bullet-}$ was first observed in the beginning. However, the spectrum of **2b**$^{\bullet-}$ gradually decreased in intensity with reduction time. The vanishing of **2b**$^{\bullet-}$ was immediately followed by the appearance of a new spectrum as shown in Figure 7a. The time evolution of the spectrum observed at −3.0 V indicates the generation of dianion diradical **2b**$^{2\bullet2-}$ at the late time. There seems to be some redox interaction between two di(6-azulenyl)-

(15) Gerson, F.; Scholz, M.; Hansen, H.-J.; Uebelhart, P. *J. Chem. Soc., Perkin Trans. 2* **1995**, 215−220.

CHART 2. Schematic Representation of the Calculated Spin Density Distributions for Anion Radicals $1b^{\bullet-}$ and $2b^{\bullet-}$ and Dianion Diradical $2b^{2\bullet2-}$

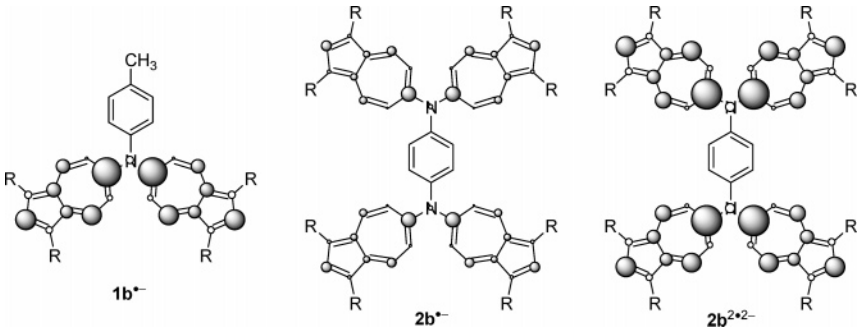

amine units of diamine **2b**, although the E_1^{red} wave is observed as a single-step, two-electron transfer in the cyclic voltammogram. The simulation using a g value of 2.0025 and hyperfine coupling constants of 0.572 (1N), 0.257 (4H), and 0.048 mT (6H) reproduced the observed spectrum of $\mathbf{2b}^{2\bullet2-}$ except the central part where some lines due to other species were still superimposed. It is interesting that the hyperfine coupling constants of diamine dianion diradical $\mathbf{2b}^{2\bullet2-}$ are the same as those of monoamine anion radical $\mathbf{1b}^{\bullet-}$, indicating the reduction of both di(6-azulenyl)amine units in $\mathbf{2b}^{2\bullet2-}$. Each hyperfine line in the ESR spectrum of $\mathbf{2b}^{2\bullet2-}$ does not show any clearly additional splittings. No further splittings mean a negligible exchange interaction between the two radicals on each di(6-azulenyl)amine unit in $\mathbf{2b}^{2\bullet2-}$. Therefore, it is concluded that one unpaired electron is delocalized within a restricted area of one di(6-azulenyl)-amine unit. B3LYP/6-31G** density functional calculation of dianion diradical $\mathbf{2b}^{2\bullet2-}$ without ester substituents also provided evidence of the observed spin density distribution (Chart 2). There are no significant differences in their geometry between the calculated structure of the anion radical and that of the dianion diradical. The dihedral angle of each ring in the dianion diradical is almost identical with that of the anion radical (see the Supporting Information). This structural similarity between the anion radical and the dianion diradical should be responsible for the facile two-electron transfer in diamines **2a**,**b** as observed by the CV measurement. The studies on the ESR of amine **1b** and diamine **2b** under electrochemical reduction conditions confirm that the radical anionic states are effectively stabilized by the resonance hybrid between two azulene rings on the di-(6-azulenyl)amine unit.

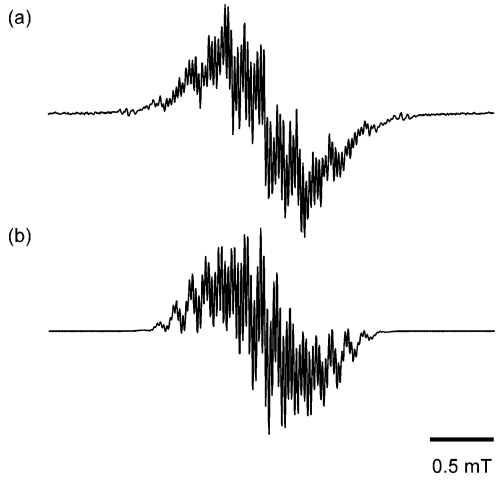

FIGURE 6. ESR spectrum of radical anion $\mathbf{2b}^{\bullet-}$ generated by the electrochemical reduction in dimethylformamide at −1.5 V at room temperature: (a) observed ESR spectrum and (b) computer simulation.

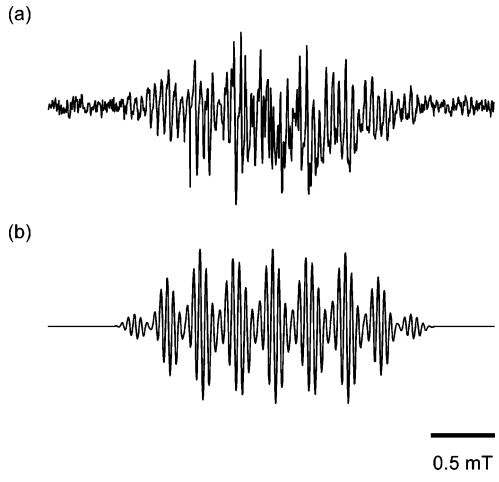

FIGURE 7. ESR spectrum of dianion diradical $\mathbf{2b}^{2\bullet2-}$ generated by the electrochemical reduction in dimethylformamide at −3.0 V at room temperature: (a) observed ESR spectrum and (b) computer simulation.

Electrochromic Analysis. Visible spectral analysis of amines **1a**,**b**, taken during electrochemical reduction, revealed gradual disappearance of the absorption bands of **1a**,**b** along with increasing new absorption maxima at 625 and 605 nm, respectively; well-defined isosbestic points at 502 and 562 nm were observed (Figure 8). The color of the solution gradually changed from red to green during the electrochemical reduction. The reverse oxidation of the green-colored solution regenerated the visible spectra of the red-colored **1a** and **1b**. As indicated by a combined ESR and visible spectral study, the species giving rise to the new absorption maxima are concluded to originate the formation of an anion radical from amines **1a** and **1b** by one-electron reduction as observed in the cyclic voltammogram.

When the visible spectra of diamines **2a**,**b** were measured under the electrochemical reduction conditions, a new absorption in the region was also gradually developed as shown in Figure 9. The color of the solution changed from red to green during the electrochemical reduction. The spectral changes of diamines **2a**,**b** should

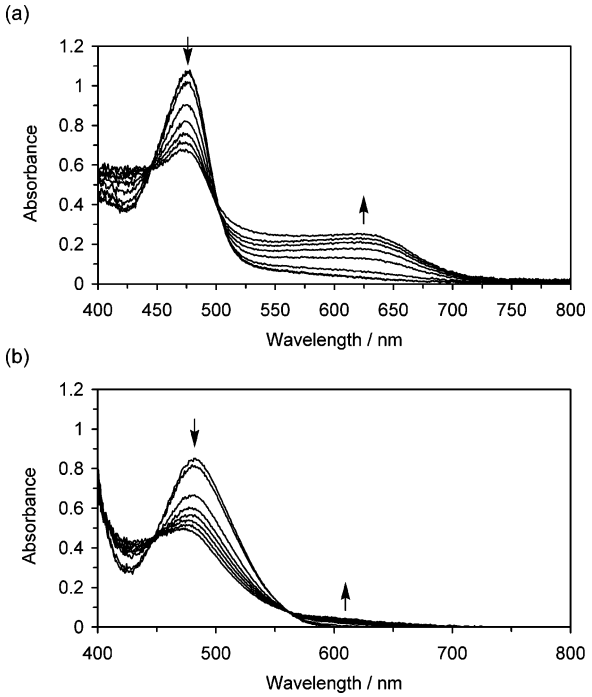

FIGURE 8. Continuous change in the visible spectrum of (a) amine **1a** (2 mL, 0.3×10^{-3} M) and (b) amine **1b** (2 mL, 0.2×10^{-3} M) in benzonitrile containing Et_4NClO_4 (0.1 M) upon constant-current electrochemical reduction (100 μA) at 5 and 1 min intervals, respectively.

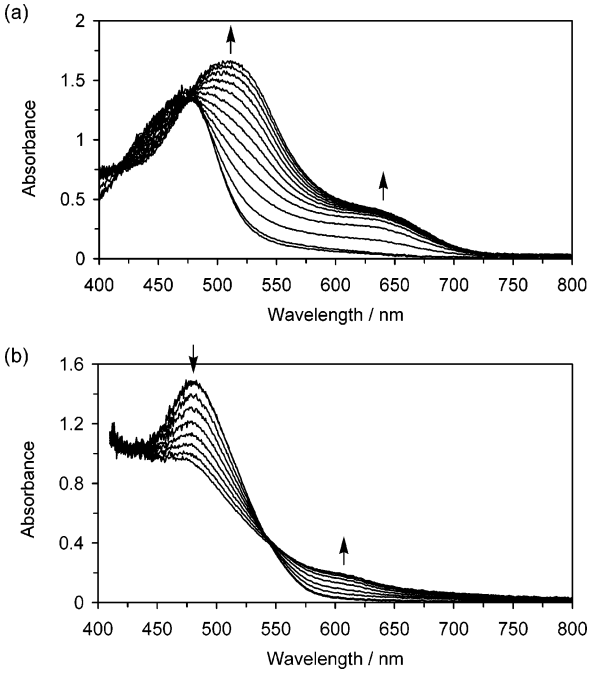

FIGURE 9. Continuous change in the visible spectrum of (a) diamine **2a** (2 mL, 0.3×10^{-3} M) and (b) diamine **2b** (2 mL, 0.5×10^{-3} M) in benzonitrile containing Et_4NClO_4 (0.1 M) upon constant-current electrochemical reduction (100 μA) at 5 and 1 min intervals, respectively.

arise from the combined formation of the anion radicals $\mathbf{2a}^{\bullet-}$ and $\mathbf{2b}^{\bullet-}$ and the dianion diradicals $\mathbf{2a}^{2\bullet2-}$ and $\mathbf{2b}^{2\bullet2-}$, taking the ESR results into consideration. The reverse oxidation of the green-colored solution of $\mathbf{2a}^{2\bullet2-}$ did not regenerate the visible spectra of the red-colored **2a**, although the reversibility was observed in the case of **2b**.

Conclusion

We have designed and synthesized a new series of azulene-substituted aromatic amines and diamines with amphoteric redox behavior, *N*,*N*-di(6-azulenyl)-*p*-toluidines **1a**,**b** and *N*,*N*,*N*′,*N*′-tetra(6-azulenyl)-*p*-phenylenediamines **2a**,**b**. Azulene-substituted aromatic amines exhibit facile electrochemical oxidation owing to the amine substituent and also show electrochemical reduction because of the generation of an anion radical stabilized by the resonance effect between the two 6-azulenyl groups. The ESR measurement of $\mathbf{1b}^{\bullet-}$, $\mathbf{2b}^{\bullet-}$, and $\mathbf{2b}^{2\bullet2-}$ generated by the electrochemical reduction conditions revealed that the unpaired electron of the anion radical delocalizes over all the azulene rings. The electorochromic property of these compounds was revealed by the measurement of spectroelectrograms. The color of the solution of **1a**,**b** and **2a**,**b** changed reversibly from red to green by electrochemical reduction, except for the case of diamine **2a**. The electrochemical investigations suggest that these compounds might be applied as an electron-transporting material along with a hole-transporting material to the optoelectronic devices.

Experimental Section

General Procedures. For general experimental details and instrumentation, see our earlier publication.[16] The detailed peak assignment of ^{1}H and ^{13}C NMR spectra was accomplished by NOE, CHCOSY, COLOC, HMQC, and/or HMBC experiments.

General Procedure for the Pd-Catalyzed Reaction of 6-Bromoazulenes 3a,b with 4 and 6. The degassed solution of 6-bromoazulenes **3a**,**b**, *p*-toluidine (**4**) or *p*-phenylenediamine (**6**), Cs_2CO_3, $Pd_2(dba)_3{\cdot}CHCl_3$, and BINAP in toluene was stirred for 1−2 days at 80 °C under an Ar atmosphere. After the mixture was cooled at room temperature, the solvent was removed under reduced pressure. The products were isolated by column chromatography on silica gel and/or gel permeation chromatography (GPC) with $CHCl_3$.

***N*,*N*-Bis(1,3-bisethoxycarbonyl-6-azulenyl)-*p*-toluidine (1b).** The general procedure was followed by using **3b** (140 mg, 0.399 mmol), **4** (21 mg, 0.20 mmol), Cs_2CO_3 (423 mg, 1.30 mmol), $Pd_2(dba)_3{\cdot}CHCl_3$ (21 mg, 0.020 mmol), and BINAP (26 mg, 0.042 mmol) in toluene (10 mL). Column chromatography on silica gel with CH_2Cl_2 and ethyl acetate and GPC with $CHCl_3$ afforded **5b** (7 mg, 9%) and **1b** (85 mg, 67%).

Data for 5b: yellow needles; mp 207.5−208.0 °C (toluene); MS (70 eV) *m*/*z* (relative intensity) 377 (M^+, 100), 332 (M^+ − OEt, 33), 305 (M^+ − CO_2Et + H, 21), 304 (M^+ − CO_2Et, 30); IR (KBr disk) ν_{max} 3303 (m, NH), 1653 (s, C=O) cm^{-1}; UV−vis (CH_2Cl_2) λ_{max} (nm) (log ϵ) 230 (4.38), 267 (4.29), 285 sh (4.12), 349 (4.71), 373 sh (4.48), 399 (4.30), 455 sh (3.70); ^{1}H NMR (500 MHz, $CDCl_3$) δ = 9.36 (d, 2H, J = 11.5 Hz, $H_{4,8}$), 8.33 (s, 1H, H_2), 7.24 (d, 2H, J = 8.3 Hz, $H_{3',5'}$), 7.18 (d, 2H, J = 8.3 Hz, $H_{2',6'}$), 7.17 (s, 1H, NH), 7.10 (d, 2H, J = 11.5 Hz, $H_{5,7}$), 4.36 (q, 4H, J = 7.1 Hz, 1,3-CO_2Et), 2.40 (s, 3H, 4′-Me), 1.40 (t, 6H, J = 7.1 Hz, 1,3-CO_2Et); ^{13}C NMR (125 MHz, $CDCl_3$) δ = 165.8 (s, 1,3-CO_2Et), 157.9 (C_6), 139.2 ($C_{4,8}$), 137.3 ($C_{3a,8a}$), 136.8 ($C_{4'}$), 136.3 (C_2), 135.4 ($C_{1'}$), 130.5 ($C_{3',5'}$), 124.5 ($C_{2',6'}$), 116.4 ($C_{5,7}$), 116.0 ($C_{1',3'}$), 59.6 (t, 1,3-CO_2Et), 21.1 (4′-Me), 14.6

(16) Ito, S.; Terazono, T.; Kubo, T.; Okujima, T.; Morita, N.; Murafuji, T.; Sugihara, Y.; Fujimori, K.; Kawakami, J.; Tajiri, A. *Tetrahedron* **2004**, *60*, 5357−5366.

(q, 1,3-CO_2Et). Anal. Calcd for $C_{23}H_{23}NO_4$: C, 73.19; H, 6.14; N, 3.71. Found: C, 73.18; H, 6.17; N, 3.65.

Data for 1b: red microneedles; mp 233.0−233.6 °C (toluene); MS (70 eV) *m/z* (relative intensity) 647 (M^+, 100); IR (KBr disk) ν_{max} 1688 (s, C=O) cm^{-1}; UV−vis (CH_2Cl_2) λ_{max} (nm) (log ϵ) 236 (4.80), 269 (4.65), 312 (4.59), 348 sh (4.56), 370 (4.66), 389 (4.66), 478 (4.59); ^{1}H NMR (500 MHz, $CDCl_3$) δ = 9.48 (d, 4H, J = 11.5 Hz, $H_{4,8}$), 8.63 (s, 2H, H_2), 7.50 (d, 4H, J = 11.5 Hz, $H_{5,7}$), 7.26 (d, 2H, J = 8.4 Hz, $H_{3',5'}$), 7.13 (d, 2H, J = 8.4 Hz, $H_{2',6'}$), 4.40 (q, 8H, J = 7.1 Hz, 1,3-CO_2Et), 2.42 (s, 3H, 4′-Me), 1.42 (t, 12H, J = 7.1 Hz, 1,3-CO_2Et); ^{13}C NMR (125 MHz, $CDCl_3$) δ = 165.0 (s, 1,3-CO_2Et), 158.3 (C_6), 143.6 ($C_{1'}$), 141.2 (C_2), 140.6 ($C_{3a,8a}$), 138.0 ($C_{4,8}$), 137.8 ($C_{4'}$), 131.4 ($C_{3',5'}$), 127.4 ($C_{2',6'}$), 126.7 ($C_{5,7}$), 117.3 ($C_{1,3}$), 60.0 (t, 1,3-CO_2Et), 21.1 (4′-Me), 14.5 (q, 1,3-CO_2Et). Anal. Calcd for $C_{39}H_{37}NO_8$: C, 72.32; H, 5.76; N, 2.16. Found: C, 72.35; H, 6.06; N, 2.00.

Reaction of *N*-(1,3-Bisethoxycarbonyl-6-azulenyl)-*p*-toluidine (5b). The general procedure was followed by using **3b** (140 mg, 0.399 mmol), **5b** (151 mg, 0.400 mmol), Cs_2CO_3 (425 mg, 1.30 mmol), $Pd_2(dba)_3$·$CHCl_3$ (22 mg, 0.021 mmol), and BINAP (27 mg, 0.043 mmol) in toluene (10 mL). Column chromatography on silica gel with CH_2Cl_2 and ethyl acetate and GPC with $CHCl_3$ afforded **1b** (194 mg, 75%) and the recovered **5b** (22 mg, 15%).

***N*,*N*-Di(6-azulenyl)-*p*-toluidine (1a).** The general procedure was followed by using **3a** (415 mg, 2.00 mmol), **4** (108 mg, 1.01 mmol), Cs_2CO_3 (2.12 g, 6.51 mmol), $Pd_2(dba)_3$·$CHCl_3$ (104 mg, 0.100 mmol), and BINAP (121 mg, 0.194 mmol) in toluene (50 mL). Column chromatography on silica gel with CH_2Cl_2 and GPC with $CHCl_3$ afforded **5a** (82 mg, 35%) and **1a** (187 mg, 52%).

Data for 5a: dark red microneedles; mp 157.5−157.9 °C (toluene); MS (70 eV) *m/z* (relative intensity) 233 (M^+, 100), 218 (M^+ − Me, 48), 217 (M^+ − Me − H, 83), 141 (M^+ − C_7H_8, 57); IR (KBr disk) ν_{max} 3403 (m, NH) cm^{-1}; UV−vis (CH_2Cl_2) λ_{max} (nm) (log ϵ) 290 sh (4.22), 317 (4.70), 401 (4.31), 494 (2.82), 628 (2.08); ^{1}H NMR (600 MHz, $CDCl_3$) δ = 8.01 (d, 2H, J = 10.9 Hz, $H_{4,8}$), 7.41 (t, 1H, J = 3.7 Hz, H_2), 7.19 (d, 2H, J = 8.0 Hz, $H_{3',5'}$), 7.14 (d, 2H, J = 8.0 Hz, $H_{2',6'}$), 7.14 (d, 2H, J = 3.7 Hz, $H_{1,3}$), 6.61 (d, 2H, J = 10.9 Hz, $H_{5,7}$), 6.26 (s, 1H, NH), 2.37 (s, 3H, 4′-Me); ^{13}C NMR (150 MHz, $CDCl_3$) δ = 154.3 (C_6), 137.1 ($C_{1'}$), 136.9 ($C_{4,8}$), 135.1 ($C_{4'}$), 134.2 ($C_{3a,8a}$), 130.2 ($C_{3',5'}$), 129.9 (C_2), 123.8 ($C_{2',6'}$), 118.7 ($C_{1,3}$), 109.8 ($C_{5,7}$), 21.0 (4′-Me); HRMS *m/z* calcd for $C_{17}H_{15}N$ 233.1199, found 233.1196. Anal. Calcd for $C_{17}H_{15}N$: C, 87.52; H, 6.48; N, 6.00. Found: C, 87.70; H, 6.56; N, 5.76.

Data for 1a: dark green plates; mp 141.0−142.0 °C (MeOH/H_2O); MS (FAB) *m/z* (relative intensity) 359 (M^+, 100); UV−vis (CH_2Cl_2) λ_{max} (nm) (log ϵ) 233 sh (4.42), 279 sh (4.59), 294 (4.64), 344 (4.53), 405 sh (4.05), 472 (4.47), 570 sh (3.23); ^{1}H NMR (600 MHz, $CDCl_3$) δ = 8.07 (d, 4H, J = 10.8 Hz, $H_{4,8}$), 7.67 (t, 2H, J = 3.7 Hz, H_2), 7.26 (d, 4H, J = 3.7 Hz, $H_{1,3}$), 7.16 (d, 2H, J = 8.2 Hz, $H_{3',5'}$), 7.09 (d, 2H, J = 8.2 Hz, $H_{2',6'}$), 6.98 (d, 4H, J = 10.8 Hz, $H_{5,7}$), 2.37 (s, 3H, 4′-Me); ^{13}C NMR (150 MHz, $CDCl_3$) δ = 156.6 (C_6), 145.1 ($C_{1'}$), 137.0 ($C_{3a,8a}$), 135.4 ($C_{4,8}$ and $C_{4'}$), 134.4 (C_2), 130.5 ($C_{3',5'}$), 126.8 ($C_{2',6'}$), 120.9 ($C_{5,7}$), 119.1 ($C_{1,3}$), 21.0 (4′-Me). Anal. Calcd for $C_{27}H_{21}N$: C, 90.22; H, 5.89; N, 3.90. Found: C, 90.24; H, 6.03; N, 3.85.

***N*,*N*,*N*′,*N*′-Tetrakis(1,3-bisethoxycarbonyl-6-azulenyl)-*p*-phenylenediamine (2b).** The general procedure was followed by using **3b** (283 mg, 0.806 mmol), **6** (22 mg, 0.20 mmol), Cs_2CO_3 (847 mg, 2.60 mmol), $Pd_2(dba)_3$·$CHCl_3$ (42 mg, 0.041 mmol), and BINAP (51 mg 0.082 mmol) in toluene (10 mL). Column chromatography on silica gel with CH_2Cl_2 and ethyl acetate and GPC with $CHCl_3$ afforded **7** (28 mg, 15%) and **2b** (47 mg, 20%).

Data for 7: red powder; mp 192.0−192.5 °C (toluene); MS (FAB) *m/z* (relative intensity) 918 (M^+, 54), 873 (M^+ − OEt, 73); IR (KBr disk) ν_{max} 3310 (w, NH), 1690 (s, C=O) cm^{-1}; UV−vis (CH_2Cl_2) λ_{max} (nm) (log ϵ) 232 (4.90), 268 (4.74), 284 sh (4.56), 305 sh (4.52), 312 sh (4.52), 368 (4.86), 424 sh (4.63), 467 (4.63); ^{1}H NMR (600 MHz, $CDCl_3$) δ = 9.53 (d, 4H, J = 11.4 Hz, $H_{4,8}$), 9.45 (d, 2H, J = 11.6 Hz, $H_{4',8'}$), 8.66 (s, 2H, H_2), 8.40 (s, 1H, $H_{2'}$), 7.52 (d, 4H, J = 11.4 Hz, $H_{5,7}$), 7.45 (s, 1H, NH), 7.37 (d, 2H, J = 8.7 Hz, $H_{3'',5''}$), 7.28 (d, 2H, J = 11.6 Hz, $H_{5',7'}$), 7.26 (d, 2H, J = 8.7 Hz, $H_{2'',6''}$), 4.40 (q, 8H, J = 7.1 Hz, 1,3-CO_2Et), 4.37 (q, 4H, J = 7.1 Hz, 1′,3′-CO_2Et), 1.43 (t, 12H, J = 7.1 Hz, 1,3-CO_2Et), 1.41 (t, 6H, J = 7.1 Hz, 1′,3′-CO_2Et); ^{13}C NMR (150 MHz, $CDCl_3$) δ = 165.5 (s, 1,3-CO_2Et), 165.0 (s, 1,3-CO_2Et), 157.9 (C_6), 155.9 ($C_{6'}$), 143.4 ($C_{1''}$ or $C_{4''}$), 141.6 (C_2), 140.7 ($C_{3a,8a}$), 139.2 ($C_{4',8'}$), 138.0 ($C_{4,8}$), 138.0 ($C_{3'a,8'a}$), 137.6 ($C_{1''}$ or $C_{4''}$), 137.4 ($C_{2'}$), 128.5 ($C_{2'',6''}$), 126.9 ($C_{5,7}$), 124.7 ($C_{3'',5''}$), 117.6 ($C_{1,3}$), 117.1 ($C_{5',7'}$), 116.5 ($C_{1',3'}$), 60.1 (t, 1,3-CO_2-Et), 59.8 (t, 1′,3′-CO_2Et), 14.6 (q, 1′,3′-CO_2Et), 14.5 (q, 1,3-CO_2-Et). Anal. Calcd for $C_{54}H_{50}N_2O_{12}$: C, 70.58; H, 5.48; N, 3.05. Found: C, 70.33; H, 5.50; N, 3.03.

Data for 2b: red powder; mp > 300 °C (toluene); MS (FAB) *m/z* (relative intensity) 1188 (M^+, 25), 1143 (M^+ − OEt, 78); IR (KBr disk) ν_{max} 1690 (s, C=O) cm^{-1}; UV−vis (CH_2Cl_2) λ_{max} (nm) (log ϵ) 237 (5.02), 267 (4.85), 298 (4.63), 318 (4.61), 348 sh (4.80), 372 (4.93), 388 (4.93), 472 (4.77); ^{1}H NMR (500 MHz, $CDCl_3$) δ = 9.59 (d, 8H, J = 11.4 Hz, $H_{4,8}$), 8.68 (s, 4H, H_2), 7.57 (d, 8H, J = 11.4 Hz, $H_{5,7}$), 7.28 (s, 4H, $H_{2',3',5',6'}$), 4.42 (q, 16H, J = 7.1 Hz, 1,3-CO_2Et), 1.44 (t, 24H, J = 7.1 Hz, 1,3-CO_2Et); ^{13}C NMR (125 MHz, $CDCl_3$) δ = 164.9 (s, 1,3-CO_2Et), 157.6 (C_6), 144.5 ($C_{1',4'}$), 141.9 (C_2), 140.9 ($C_{3a,8a}$), 138.2 ($C_{4,8}$), 128.6 ($C_{2',3',5',6'}$), 127.3 ($C_{5,7}$), 117.7 ($C_{1,3}$), 60.1 (t, 1,3-CO_2Et), 14.6 (q, 1,3-CO_2Et). Anal. Calcd for $C_{70}H_{64}N_2O_{16}$: C, 70.70; H, 5.42; N, 2.36. Found: C, 70.33; H, 5.61; N, 2.33.

***N*,*N*,*N*′,*N*′-Tetra(6-azulenyl)-*p*-phenylenediamine (2a).** The general procedure was followed by using **3a** (166 mg, 0.802 mmol), **6** (21 mg, 0.19 mmol), Cs_2CO_3 (849 mg, 2.61 mmol), $Pd_2(dba)_3$·$CHCl_3$ (42 mg, 0.041 mmol), and BINAP (49 mg, 0.079 mmol) in toluene (10 mL). Column chromatography on silica gel with CH_2Cl_2 and GPC with $CHCl_3$ afforded **2a** (24 mg, 20%): dark red powder; mp > 300 °C (toluene); MS (FAB) *m/z* (relative intensity) 613 (M^+ + H, 7), 612 (M^+, 4); UV−vis (CH_2Cl_2) λ_{max} (nm) (log ϵ) 233 (4.75), 287 (4.93), 338 (4.92), 441 sh (4.69), 469 (4.76); ^{1}H NMR (600 MHz, $CDCl_3$) δ = 8.14 (d, 8H, J = 10.8 Hz, $H_{4,8}$), 7.71 (t, 4H, J = 3.7 Hz, H_2), 7.30 (d, 8H, J = 3.7 Hz, $H_{1,3}$), 7.14 (s, 4H, $H_{2',3',5',6'}$), 7.05 (d, 8H, J = 10.8 Hz, $H_{5,7}$); ^{13}C NMR (150 MHz, $CDCl_3$) δ = 156.0 (C_6), 144.3 ($C_{1',4'}$), 137.2 ($C_{3a,8a}$), 135.5 ($C_{4,8}$), 135.0 (C_2), 127.2 ($C_{2',3',5',6'}$), 121.2 ($C_{5,7}$), 119.4 ($C_{1,3}$). Anal. Calcd for $C_{46}H_{32}N_2$: C, 90.16; H, 5.26; N, 4.57. Found: C, 89.80; H, 5.57; N, 4.42.

Spectroelectrogram Measurements. Sample solutions were prepared by dissolving amines **1a**,**b** and diamines **2a**,**b** in benzonitrile containing Et_4NClO_4 (0.1 M) and were degassed through an Ar stream. Spectroelectrogram measurements of amines **1a**,**b** and diamines **2a**,**b** were carried out using a quartz cell (1 × 10 × 35 mm) equipped with a Pt mesh and a wire as the working and counter electrodes, respectively, which were separated by a glass filter. The electrical current was monitored by a microampere meter. Spectroelectrograms were measured on a fiber optic spectrometer at 1 or 5 min intervals.

Acknowledgment. The present work was supported by Grants-in-Aid for Scientific Research (No. 14540486 to S.I. and No. 15310069 to T.I.) from the Ministry of Education, Culture, Sports, Science, and Technology, Japan.

Supporting Information Available: Reduction and oxidation waves of **1a**,**b**, **2a**,**b**, and **5a**,**b**, DPVs of **1a**,**b** and **2a**,**b**, ^{1}H NMR spectra of **1b**, **2b**, **5b**, and **7**, optimized structure with HOMOs and LUMOs of **1a** without the 4′-methyl group, and optimized structures with spin density distribution of anion radicals $\mathbf{1a}^{\bullet-}$ and $\mathbf{2b}^{\bullet-}$ and dianion diradical $\mathbf{2b}^{2\bullet2-}$ (PDF). This material is available free of charge via the Internet at http://pubs.acs.org.

JO048489S